MADRID
inter.noise 2019
June 16 - 19
NOISE CONTROL FOR A BETTER ENVIRONMENT

The Attenuation of Flow-Induced Cavity Noise in a Wind-Tunnel by Micro-Perforations

Maury, Cédric[1]
Laboratory of Mechanics and Acoustics (CNRS LMA), Ecole Centrale Marseille
4 impasse Nikola Tesla, 13013 Marseille, France

Bravo, Teresa[2]
Consejo Superior de Investigaciones Cientificas (CSIC)
Serrano 144, 28006 Madrid, Spain

Mazzoni, Daniel[3]
Institut de Recherche sur les Phénomènes Hors Equilibres (IRPHE), UMR–CNRS
38 rue Frédéric Joliot-Curie, 13013 Marseille, France

ABSTRACT

Experimental studies have been carried out to assess the effect on the pressure fluctuations of micro-perforating the base wall of cavities mounted in a low-speed wind-tunnel and undergoing a fully-developed turbulent boundary layer. Measurements in transitional- and closed-flow regimes showed a reduction by up to 8 dB of the dominant tonal peaks in the base wall-pressures. These peaks occur on one-third of the cavity floor towards the leading edge. They are identified as transverse tunnel-cavity resonances excited by the shear layer and coupled with the thin panel flexural modes. However, the micro-perforations are inefficient downstream of the attenuation zone to attenuate the broadband pressure fluctuations. Two-dimensional Lattice-Boltzmann simulations were performed for a transitional cavity mounted in a waveguide and undergoing a low-speed boundary layer. The calculated wall pressure spectra confirmed the existence of transverse tunnel-cavity resonances as well as their attenuation at the base and at the mouth of the cavity by inserting a micro-perforated floor. In particular, the dissipation of energy is concentrated within and at the inlet-outlet of the base-wall apertures which correspond to regions of maximum velocity fluctuations.

Keywords: Micro-perforated panels; flow cavity; Lattice-Boltzmann simulations.
I-INCE Classification of Subject Number: 35
http://i-ince.org/files/data/classification.pdf

[1]cedric.maury@centrale-marseille.fr
[2]teresa.bravo@csic.es
[3]daniel.mazzoni@centrale-marseille.fr

1.INTRODUCTION

The noise generated by a flow passing over a shallow cavity is a subject of considerable importance for the transportation industry. Considering aircraft noise abatement technologies, the reduction of jet noise has brought attention towards the airframe noise that is predominant under approach condition at Mach 0.2 [1]. Landing gears, high-lift flaps and slats are amongst the major contributors to the cavity flow-induced noise. Flow noise issues also appears in pantograph cavities of high-speed trains [2], in automotive door seals [3] and in open sunroofs [4].

The present work deals with the control of flow-induced pressure fluctuations in cavities using unbacked micro-perforated panels (MPPs). Applications concerning this subject include deployable low-noise high-drag perforated spoilers mounted on aircraft wings [5], perforated cladding panels wrapped around buildings to control light level exposure but prone to generate wind-induced noise over the facade cavities [6] and MPPs inserted within double-glazed ventilation window systems [7]. The objective is to examine the effect of a micro-perforated base wall on the attenuation of the pressure fluctuations induced by a low-speed flow over cavities in transitional regime.

Mathematical model have to take into account not only the shear layer parameters but also the geometrical factors of the cavity, in particular the cavity length-to-depth ratio, L/D. Flow cavities have been classified depending on this ratio into three categories [8]. Closed flows have been observed in elongated cavities with a large aspect ratio $L/D \geq 13$. Although longitudinal modes appear to be driven by the shear layer instability, self-sustained oscillations do not occur in this regime with typical broadband noise generated in the far-field. Also, the shear layer reattaches and separates at some point on the cavity base wall. Examples are found in solar collectors surrounded by wind barriers to improve their thermal efficiency [9]. On the other hand, open flow cavities are characterized by a ratio $L/D \leq 8$. In this case, the shear layer spans the whole cavity length. For $L/D \leq 4$, it is prone to generate intense acoustic tones at discrete frequencies induced by the coincidence between the cavity self-sustained oscillations and the acoustical resonances [10]. Such typical configurations are observed in landing gears and high lift devices during aircraft approach. The intermediate configuration, $8 \leq L/D \leq 13$, is denoted transitional. This flow regime has been scarcely studied. It exhibits both tonal and broadband components in the measured sound pressure spectra, but their relative importance depends on each specific configuration [11].

Knowledge of these physical processes is of major importance for flow noise control reduction. Many active techniques have been considered as a suitable option to reduce flow cavity noise. They aim at producing minute variations of the mass flow rate in the cavity that affect the spatial coherence of the shear layer. They have been performed with several types of actuators: piezoelectric arrays, oscillating vortex generators, synthetic jets and fluidic oscillators. Most of them have been fixed side by side in the region of flow maximum receptivity, e.g. on the upstream wall of the cavity to add small periodic velocity fluctuations to the shear layer. It was found that a cost-efficient strategy is phase control, e.g. to generate velocities and surface pressure waves in opposite-sign between adjacent actuators so that their contributions cancel out far away from the cavity [12]. It should be indicated that all these techniques are mainly studied on downscaled cavity models and considerations for aviation safety and energy consumption have to be taken into account before being applied to real problems.

Passive attenuation techniques have also been investigated, although to a lesser extent. They consist of using sloped floors [13] or inserting spanwise cylinders within the cavity to create or break large recirculation bubbles [14]. One may also round the cavity downstream corner [15], change the external source of momentum with stationary screens [16] or fix small blocks at the leading edge [17] to produce a vertical displacement of the shear layer past the cavity, thereby reducing the interaction with the downstream edge corner. Passive liners, widely used for instance in aircraft nacelles to control fan and jet noise, allow noise sources to be reduced in an optimised frequency band, but they cannot efficiently suppress a large number of acoustic modes unless massive and thick partitions are installed [1]. Another important drawback is that, when used over the fuselage, they may affect the aerodynamic performance of the airplane by increasing the drag [18]. Furthermore, when applied to flow noise cavity problems, they might not necessarily be compatible with operational procedures as filling fuselage cavities with such treatment may make them non functional. It is then necessary to find a compromise between aerodynamic performance, functionality and noise reduction issues that could be fulfilled by the use of thin micro-slit or micro-perforated panels.

Rigidly-backed MPPs have been proposed initially in the area of architectural acoustics as Helmholtz-type resonators that improve sound absorption in the low-medium frequency range [19, 20]. They can also be unbacked and located well inside a cavity to dampen a handful of specific acoustic modes as it would be the case for the treatment of boiler tones in heat-exchanger cavities [21]. They have also been used to damp the first spinning modes when located parallel to the axis of an air conditioning duct [22].

The objective of this work is to propose a low drag passive strategy using MPPs in order to attenuate low-speed flow-induced noise over transitional cavities. The behaviour of MPP devices when exposed to grazing and bias flows such as plugged MPP silencers is a subject of current research. A previous work [23] considered a classical arrangement made up of a flush-mounted MPP backed by a cavity and exposed to a fully-developed turbulent boundary layer (TBL). It was shown that a large part of the power injected by the aerodynamic pressures into the MPP was efficiently dissipated and transmitted through the apertures provided that the hole-based Strouhal number, $\mathrm{St}_h = fd_h/U_\infty$, stayed lower than 0.1, with f the frequency, d_h the holes diameter and U_∞ the flow free-stream velocity. An alternative configuration is studied in this work with an unbacked MPP constituting the base wall of a shallow transitional cavity mounted in a low-speed wind tunnel. An extensive set of experimental data are presented and analysed in Section 2, followed by a numerical study in Section 3, with recommendations for the design and selection of the best configurations for the flow-cavity noise attenuation. We will finish outlining the main conclusions and some recommendations for future work.

2. EXPERIMENTAL CHARACTERIZATION

Experiments have been performed in the closed-loop S1 wind-tunnel of the IRPHE Fluid Dynamics Laboratory ("Institut de Recherche sur les Phénomènes Hors Equilibre", Marseille, France) in order to determine the effect of micro-perforating the base wall of shallow cavities on the flow noise induced by a low speed TBL. A schematic of the experimental system is shown in Fig. 1. Pictures of the MPP

constituting the base wall of the cavity mounted on the top of the test section can be seen in Figs. 1(b) and 2(b).

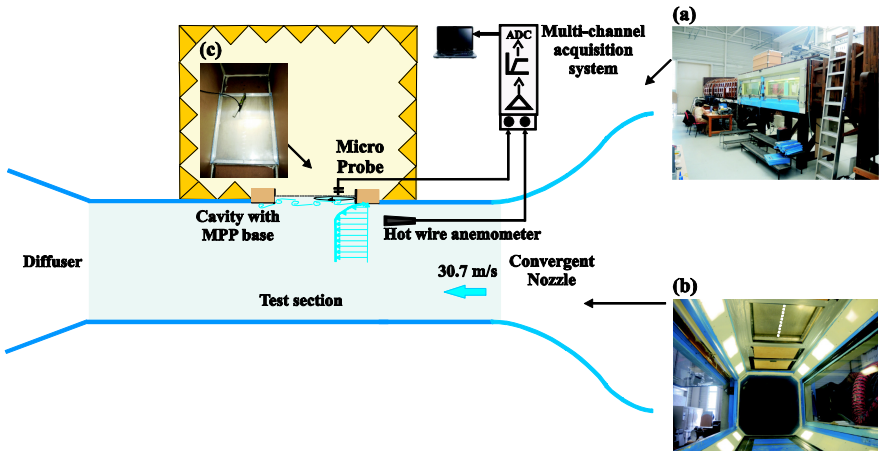

Fig. 1. Sketch of the experimental set-up to measure wall-pressures upstream and on the base of flow cavities: (a) overall view of the IRPHE low-speed wind-tunnel facility; (b) inner view of the wind-tunnel test section on top of which is mounted the shallow transitional cavity: the white points over the cavity base wall correspond to the measurements positions; (c) view from the base no-flow side of the micro-probe pressure sensor used to measure the wall-pressure fluctuations on the cavity floor.

2.1 Measurements in the wind-tunnel for the TBL characterization

The test section is located between the convergent nozzle and the diffuser. It is 7 m long, has a square cross-section of $0.9\,\mathrm{m}\times0.9\,\mathrm{m}$ and is insulated from the fan section by several silencers located upstream and downstream from the fan. The 11 blades fan generates at 400 revolutions per minute a free-stream velocity of $30.7\,\mathrm{m\,s^{-1}}$ in the test section. It is known to produce acoustic contamination at 73 Hz, the blade passing frequency. A laminar airflow is accelerated through the convergent from a settling chamber filled with honeycomb straighteners. A sandpaper strip was fixed crossflow on the top wall 2.5 m upstream the test section in order to efficiently trig the airflow transition to turbulence. Before analysing the MPP performance, it is of interest to well-characterize the nature of the incoming flow since it greatly influences the properties of the cavity noise.

Aerodynamic measurements were performed at $U_\infty = 30.7\,\mathrm{m\,s^{-1}}$ with a calibrated DANTEC 55P11 hot-wire probe to measure the mean and fluctuating parts of the flow velocity at 1 cm ahead from the cavity upstream edge and at several stand-off distances from the upstream wall. The mean flow velocity profile, $\overline{U}/U_\infty$, followed a seventh power law of z/δ with δ the boundary layer thickness ($\delta = 0.052\,\mathrm{m}$ at $30.7\,\mathrm{m\,s^{-1}}$). The boundary layer shape factor, δ^*/θ, was found to be nearly equal to 1.28 for each flow velocity, with the boundary layer displacement and momentum thicknesses respectively equal to $\delta^* = 0.006\,\mathrm{m}$ and $\theta = 0.0047\,\mathrm{m}$. These velocity profiles indicate that a fully-developed TBL was established without pressure gradient at the axial position where the shallow cavity was mounted.

Wall-pressure measurements were also performed of the point- and cross-power spectral densities between two pinhole microprobes GRAS 40SC, flush-mounted on a rigid wall ahead of the cavity. One reference probe was at a fixed point and the other

one was sequentially displaced over 40 streamwise and 20 spanwise positions, uniformly distributed and separated by $0.005\,\mathrm{m}$. The spatially-averaged point-power spectra collapsed over a single curve. In accordance with Goody's model [24], they showed a spectral decay that varied as $\omega^{-0.7}$ above 100 Hz at the onset of the mid-frequency region, e.g. in outer scaling variables for $\omega\delta/u_\tau \geq 100$ with $u_\tau = 1.2\,\mathrm{m\,s^{-1}}$ the friction velocity at $30.7\,\mathrm{ms^{-1}}$. An overall good agreement was also found between the measured and Corcos-type [25, 26] cross-correlation functions associated to the TBL wall-pressures along the spanwise and streamwise directions. However, the Corcos empirical coefficients had to be updated and made frequency-dependent for the true correlation lengths not to be over-estimated, especially at low frequencies. These results show that the TBL wall-pressures ahead of the shallow cavity are stationary and spatially homogeneous. They comply with the assumption of an incoming fully-developed TBL without pressure gradient, as already found from the in-flow aerodynamic measurements.

2.2 Pressure fluctuations induced by the TBL

A set of measurements has been carried out in the wind tunnel test section to evaluate the effect of micro-perforating the base wall of a rectangular shallow cavity on the wall-pressures induced by a low-speed TBL. As seen in Fig. 2, the cavity was mounted on the top wall of the test section. The base wall has dimensions $L \times W = 0.53\ \mathrm{m} \times 0.41\ \mathrm{m}$ respectively along the streamwise and spanwise directions. It is an aluminium panel, 1 mm thick, with a Young's modulus of $6.9\times10^{10}\,\mathrm{Nm^{-2}}$, a mass density of $2700\,\mathrm{kg\,m^{-3}}$ and a Poisson ratio of 0.33. The panel modal damping ratio was previously identified to be 1% from laser vibrometer measurements [23].

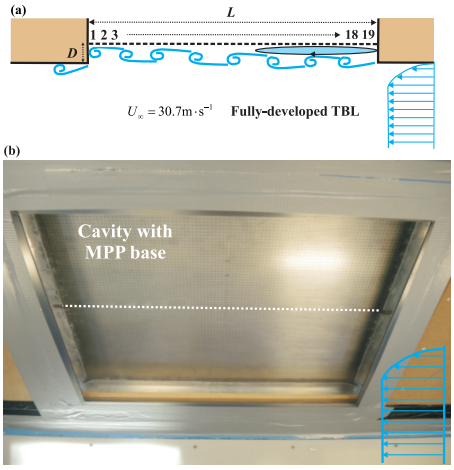

Fig. 2. (a) sketch of a transitional flow cavity with micro-perforated base wall beneath a fully developed turbulent boundary layer; (b) photography of the wind tunnel test section on top of which is mounted the micro-perforated cavity: the white points over the cavity base correspond to the 19 wall-pressure measurements positions ordered as indicated in Fig. 2(a).

The reference configuration considers a plain cavity base wall. In a second test, the plain wall is substituted by a microperforated panel with circular holes of diameter $d_h = 0.5\,\mathrm{mm}$, perforation ratio $\sigma = 0.8\%$ and a separation distance between the holes

axis of 5 mm. A picture of the microperforated base is shown in Fig. 2(b) for a transitional cavity of length-to-depth ratio $L/D_T = 10.6$ with a depth $D_T = 0.05\,\mathrm{m}$. Given a free-stream velocity set to $30.7\,\mathrm{m\,s^{-1}}$, the transitional flow experiments were performed at a Reynolds number, $\mathrm{Re}_T = U_\infty D_T/\nu$, equal to $9.8\,10^4$ with $\nu = 1.57\,10^{-5}\ \mathrm{m^2 s^{-1}}$ the air kinematic viscosity at 20°C. The panels edges were glued on four supporting steel-made vertical frames of width 1 cm so that clamped boundary conditions were replicated in both configurations.

Because we are interested on the reduction of the impinging aerodynamic wall-pressures by the sole microperforate, the cavity base wall was unbacked during the measurements. The MPP no-flow side thus radiates into an enclosure, 1.4 m long, 0.5 m wide and 0.8 m high, whose honeycomb sandwich walls have been designed to insulate the radiating area from the external fan blade passing frequency (15 dB reduction at 73 Hz). Wall-pressure measurements were performed using a pinhole microphone GRAS 40SC with probe diameter 1.25 mm and length 20 mm. According to Schewe measurements [27], an ideal transducer should have a diameter lower than 20 times the viscous length scale, ν/u_τ, for the wall-pressures to be solely influenced by the viscous and buffer layers in the inner wall region. The microprobe diameter is about 5 times greater so that it may also capture the influence of the log-law region. The short probe length provides a flat frequency-response and wave-pressure losses in the thin tube lower than 0.8 dB between 100 Hz and 3 kHz. During the experiment, the probe millimetric tip was sequentially inserted into small holes of diameters 1.27 mm located at 19 positions evenly distributed along a lengthwise line on the cavity base. The measurement positions are separated by a distance of 0.028 m and are represented by white dots in Figs. 1(b) and 2(b). In Fig. 2(a), they are numbered from 1 to 19, the first (resp. last) points being at 0.014 m from the cavity rear (resp. front) edges. The measurement line was set at 0.2 m from the cavity side edge in order not to coincide with a line of microperforations. Therefore, it is almost a midline of the cavity width. Fig. 1(c) shows the microprobe at position 1 from within the enclosure.

Special care has been taken to ensure that the microprobe tip was mounted as flush as possible at all the measurement positions. As shown in Fig. 1(c), it was fixed onto a bar whose depth was such that submillimetric protrusion of the tip in the flow was avoided. This event was easily detected due to a significant broadband increase of the r.m.s. wall-pressures induced by the flow-tip interaction. Tip recess within the 1 mm panel thickness was also avoided so that departure from flushness did not exceed 0.1 mm.

2.3 Measurements with a rigid section

Variations of the wall-pressure point-power spectral densities along the 19 floor positions are shown in Fig. 3 for plain and microperforated cavity floors, respectively. In either case, the random components are more intense towards the rear wall of the cavity (blue curves), e.g. beyond the first recirculation zone that ends up at about 18.2 cm from the leading edge, whereas tonal components emerge towards the front wall beneath the recirculation zone (red curves). As the observation point gets closer to the upstream wall, one observes an overall decay of the wall-pressure SPLs with a clear emergence of tonal peaks above the broadband components for the plain floor case, as seen in Fig. 3(top).

The resonance peaks observed in the experiments involve a non-symmetric cavity confined within the wind-tunnel waveguide that significantly modifies the complex resonant frequencies of an unconfined cavity in the sense that acoustic

radiation losses now occur through the cut-on tunnel (T) modes. The transverse tunnel-cavity (TC) modes have a cut-on frequency lower than that of the corresponding tunnel modes. For non-symmetric cavities under a subsonic flow, as it is the case in this study, Alvarez and Kerschen [28] showed the existence of "nearly trapped" global modes with small radiation leakage and high amplitude in the TC section. This dominant mode behavior typically occurs in frequency windows bounded by the cut-on frequencies of a TC mode and of the corresponding T mode. These transverse modes have been observed experimentally and numerically in a pipe as acoustic diametral modes excited by a shear layer past an axisymmetric cavity for $M_\infty \leq 0.4$ [29].

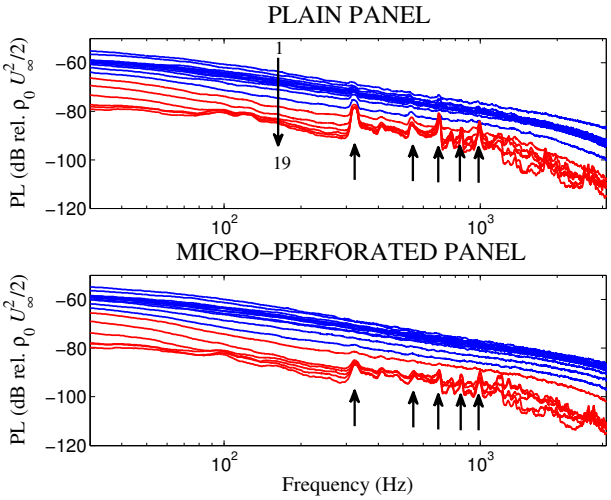

Fig. 3. Effect of microperforating the base of a transitional flow cavity ($L/D_T = 10.6$, $U_\infty = 30.7\ ms^{-1}$) on the pressure levels (PL) measured at 19 observation points evenly distributed along the centered line of the plain (top) or microperforated (bottom) base (blue: broadband components, points 1 to 13; red: tonal components, points 14 to 19).

The measured frequencies of the dominant peaks are observed in Fig. 3(top) in relation to the TC and T transverse modes resonance frequencies of the test section together with their modal orders. Apart from the first-order resonance that is not detected, the higher-order transverse resonances up to $n_z = 6$ systematically occur below the expected range of frequencies bounded by the TC and T transverse resonance frequencies, respectively given by $f_{n_z,TC} = n_z c_0/(H + D_T)$ and $f_{n_z,T} = n_z c_0/H$ with H the height of the tunnel test section. This is due to coupling with the thin panel flexural modes.

2.4 Measurements with the unbacked micro-perforated panel

In this section, we present the comparison results when perforating the floor of a transitional cavity at two different locations, 16.8 cm and 8.4 cm, apart from the upstream edge. The tonal components outlined in the previous section are clearly seen in Fig. 4(right) on the wall-pressure spectrum measured on the plain cavity floor (solid curve) at 8.4 cm from the upstream edge well beneath the recirculation bubble. It is appreciated that the presence of the MPP panel has a positive effect. Indeed, microperforating the base wall of the cavity in transitional flow regime reduces by up to 8 dB the amplitudes of these first peaks between 300 Hz and 2 kHz. It is hypothesized that a large airframe relative normal velocity then damps the TC transverse modes. The

dissipation would occur either through viscous effects within the micro-holes or through vorticity shedding at the micro-holes inlet or outlet.

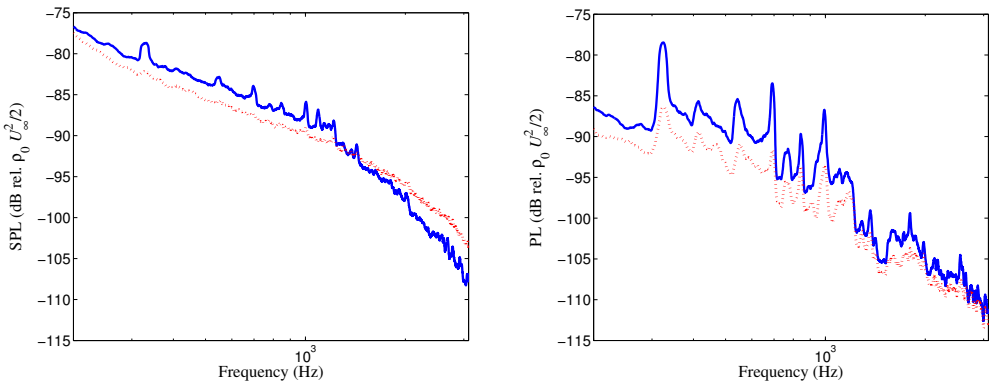

Fig. 4. Effect of a microperforated floor on the pressure level spectra measured over the base wall of a transitional cavity ($L/D_T = 10.6$): (left) at 16.8 cm and (right) at 8.4 cm from the cavity upstream edge; the solid curves correspond to a plain floor and the dotted curves to a microperforated floor.

Fig. 4(left) shows that the broadband components of the wall-pressures become preponderant towards the downstream edge so that the MPP is then less efficient for reducing the dominant peaks with only a 3 dB reduction on the first peak. One also observes in Fig. 4(left) that the interaction between the flow and the base wall micro-perforations generates excess broadband wall-pressures above 1.2 kHz. Figure 5 shows the spatial extent over which the measured wall-pressures are dissipated by the microperforations. Results are presented at one dominant peak and at a peak seen in Fig. 4(right) at 1800 Hz.

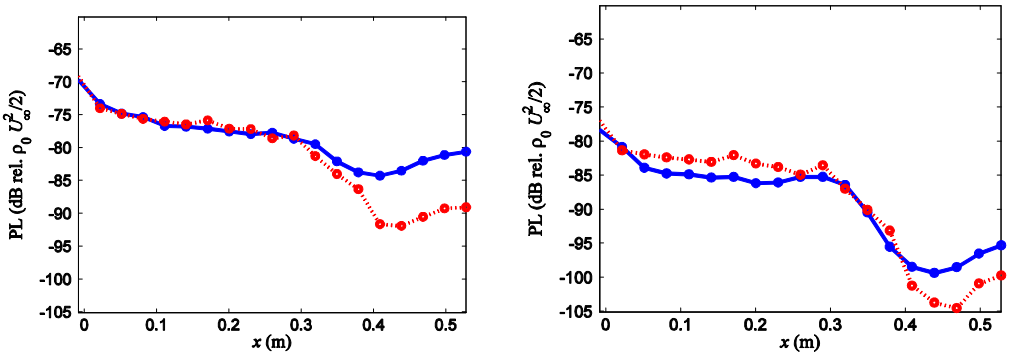

Fig. 5. Effect of a microperforated floor on the spatial distribution of the pressure levels measured along 19 observation points over the base wall of a transitional cavity ($L/D_T = 10.6$) at: 690 Hz (left) and 1800 Hz (right); the solid curves correspond to a plain floor and the dotted curves to a microperforated floor.

For these frequencies, one consistently observes an attenuation zone that occupies about one third of the cavity length towards the upstream edge. It corresponds to the size of the recirculation zone. Further downstream, the wall-pressures are dominated by the broadband pressure components over the two-thirds of the cavity

length. The MPP is then inefficient to attenuate the wall-pressure fluctuations in this zone. It even generates extra noise, up to 5 dB at 1800 Hz [see Fig. 5(right)], due to back-scattering of the aerodynamic wall-pressures as frequency increases. Although not shown, one also observed at higher frequencies a further reduction of the attenuation zone. Thus, a strategy for reducing the bottom wall-pressures in a cavity in transitional flow regime could consider a semi-microperforated floor in which only part of the floor beneath the recirculation zone would be micro-perforated in order to achieve attenuation of the dominant peaks without enhancing the aerodynamic wall-pressures further downstream.

3.NUMERICAL STUDY

The experimental set-up has been numerically modelled for the prediction of the flow cavities acoustic resonances by microperforated base walls using the Lattice Boltzmann Method (LBM). A two-dimensional LBM model has been implemented in the open access Palabos code to predict the measured attenuations.

3.1 Lattice Boltzmann modelling

The LBM is an alternative cost-efficient CFD (Computational Fluid Dynamics) approach for simulating complex multicomponent and multiphase gas flows. Instead of discretizing the macroscopic Navier-Stokes equations, it tracks the evolution of discretized particle velocity distribution functions (PVDF) defined at mesoscopic scales. The PVDF satisfies the Boltzmann kinetic equation with a suitable collision operator [30]. The fictitious particles are defined at each node of the computational domain with restricted advection and collision rules in order to recover the weakly-compressible Navier-Stokes equations. In the present study, the 2D LBM is implemented on a square lattice structure with nine neighboring lattice nodes, also termed the D2Q9 lattice Boltzmann scheme.

LBM simulations were performed on a flow cavity model in which a laminar boundary layer is incoming from the inlet section with a free-stream velocity of $30.7\,\mathrm{m\,s^{-1}}$ towards the mouth of a transitional cavity with depth $D_T = 0.05\,\mathrm{m}$ and length $L = 0.53\,\mathrm{m}$. The cavity floor of thickness 1 mm is rigid as well as the cavity side walls and the leading and trailing edges. The cavity floor is either plain or microperforated with sharp-edged apertures of width $d_h = 0.5\,\mathrm{mm}$, so that the ratio of the aperture half-width to the viscous boundary layer thickness, $\mathrm{Sh} = d_h\sqrt{\rho_0\omega/4\eta}$, is the same as in the experiment. However, the apertures have a larger separation distance $u_h = 6.25\,\mathrm{cm}$ in order to keep the same perforation ratio $\sigma_{2\mathrm{D}} = d_h/u_h = 0.8\,\%$ than in the experiment $\sigma_{\mathrm{exp.}} = \pi d_h^2/\left(4u_h^2\right) = 0.8\,\%$. The temporal and spatial resolution in the tunnel and cavity domains (without perforations) was set to $\Delta t = 6.33\,10^{-6}\,\mathrm{s}$ and $\Delta x = \Delta z = 50\ \mu\mathrm{m}$, which provided a numerical error in the speed of sound, $c_0 = 340\,\mathrm{m\,s^{-1}}$ in physical units, lower than 1% in the 8 directions of the D2Q9 scheme.

3.2 Numerical results for a micro-perforated floor

Figure 6 shows the simulated effect of microperforating the floor of a cavity in transitional flow regime on the levels of the pressure fluctuations. The pressure levels have been calculated respectively over the base wall and at the mouth of the cavity. Transverse global modes are well predicted by the 2D LBM. They occur in a frequency range limited by the cut-on frequencies of a TC mode and the corresponding tunnel mode. The first dominant peak is predicted at 703 Hz. It is intermediate between the

first TC and tunnel resonances, respectively at $f_{1,TC} = c_0/2(H + D_T) = 694\,\text{Hz}$ and at $f_{1,T} = c_0/(2H) = 708\,\text{Hz}$. The second dominant peak occurs at 1391 Hz which is in-between the second TC and tunnel resonances.

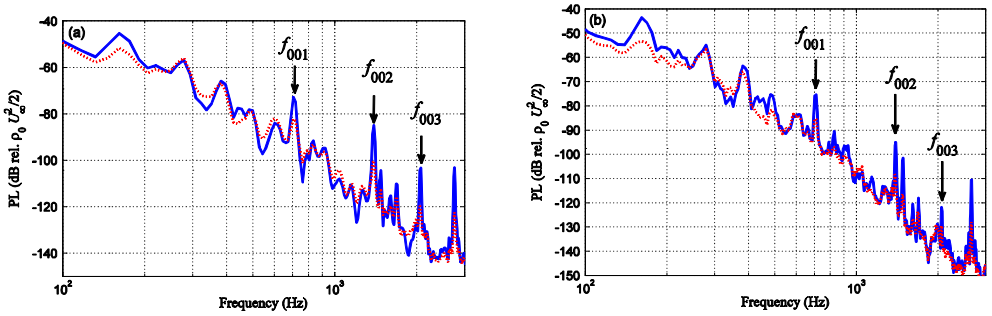

Fig. 6. Effect of a microperforated cavity floor on the pressure level spectra calculated by LBM at a horizontal distance 8.4 cm from the upstream edge: (left) over the base wall and (right) at the mouth of the cavity; the black curves correspond to a plain floor and the grey curves to a microperforated floor.

It can be seen from Figs. 6 (left) and (right) that the model captures the effect of the microperforations, e.g. to attenuate the pressure fluctuations at the floor and at the mouth of the cavity. For sake of convergence, a criterion of 80 cells per aperture width led to a number of 15 cells across the orifice viscous boundary layer at 703 Hz ($\text{Sh} = 4.2$), 10 cells at 1391 Hz ($\text{Sh} = 6$) and 8 cells at 2083 Hz ($\text{Sh} = 7$). The levels of attenuation for the pressure fluctuations at the cavity floor [Fig. 6(left)] reach 10 dB at 703 Hz and 16 dB at 1391 Hz and 2083 Hz. At the cavity mouth [Fig. 6(right)], they are lower and amount to 9 dB at 703 Hz, 13 dB at 1391 Hz and 7 dB at 2083 Hz. They overestimate the measured modal attenuations that were not exceeding 8 dB on the second transverse mode at the cavity floor. Note that the simulated boundary conditions are more conservative with respect to the experimental ones.

4. CONCLUSIONS

In this work, numerical and experimental studies have been carried out to evaluate the effect of microperforating the base wall of shallow cavities to reduce their tonal and broadband noise components under a low-speed TBL. This passive strategy has been hardly studied in shallow cavities with length-to-depth ratios of the order of 10, for which flow reattachment might occur at the cavity floor. Measurements of wall-pressure spectra performed at Mach 0.09 at the bottom of a transitional flow cavity with a length-to-depth ratio 10.6 showed dominant peaks on one third of the cavity floor towards the leading edge. Broadband pressure fluctuations dominate further downstream, with an amplitude about 10 dB above that of the first peak. The peaks are identified as transverse Tunnel-Cavity resonances excited by the shear layer and coupled with the thin panel flexural modes. Wind-tunnel measurements showed that micro-perforating the cavity floor of transitional and closed cavities significantly attenuates the amplitude of the “fluid-resonant” oscillations driven by the broadband energy of the incoming TBL. In particular, a micro-perforated floor in a transitional cavity provides up to 8 dB attenuation on the first peak levels. Out of this zone, the MPP is inefficient to reduce the broadband pressure components.

Aeroacoustic simulations based on two-dimensional Lattice Boltzmann modelling have been performed to relate the attenuation of the cavity acoustic resonances to vorticity and velocity fluctuations within the cavity and across the MPP. The calculated base-wall pressure spectra display dominant peaks due to transverse TC resonances excited by the shear layer. Assuming a number of 80 cells per aperture width (0.5 mm), the model predicts an attenuation of the dominant peaks at the floor and at the mouth of the cavity. It shows that the dissipation of energy occurs at the regions of maximum velocity fluctuations induced by well-established outflow conditions within and at the inlet-outlet of the base wall apertures.

5. ACKNOWLEDGEMENTS

This work has been funded by The Ministerio de Economía y Competitividad in Spain, project TRA2017-87978-R, AEI/FEDER, UE, "Programa Estatal de Investigación, Desarrollo e Innovación Orientada a los Retos de la Sociedad". It was supported in France by the Labex Mechanics and Complexity AAP2 managed by the Excellence Initiative Programme of Aix-Marseille University (A*MIDEX).

6. REFERENCES

1. L. Leylekian, M. Lebrun and P. Lempereur, "An *overview of aircraft noise reduction technologies*", Aerospace Lab Journal, 7, 1–14 (2014).
2. C. Noger, J. C. Patrat, J. Peube, J. L. Peube, Aeroacoustical study of the TGV pantograph recess, Journal of Sound and Vibration 231, 563–575 (2000).
3. X. Gloerfelt, Noise from automotive components, in Aerodynamic Noise from Wall-Bounded Flows, Von Karman Institute Lectures Series, Rhode-Saint-Genèse, Belgium, 2009.
4. D. Ricot, V. Maillard and C. Bailly, Numerical simulation of the unsteady flow past a cavity and application to the sunroof buffeting, 7th AIAA/CEAS Aeroacoustics Conference, Maastricht, The Netherlands, AIAA paper 2001-2112, 2001.
5. K. D. Sakaliyski, J. I. Hileman, Z. S. Spakovsky, Aero-acoustics of perforated drag plates for quiet transport aircraft, in: Proceedings of the 45th AIAA Aerospace Science Meeting and Exhibit, Reno, Nevada, U.S.A., January 2007, AIAA 2007-1032.
6. K. Tanner, N. Mackenzie, R. Jones, Y.-K. Lee, Aeroacoustic assessment of facades, in: Proceedings of Acoustics 2016, the 2nd Australasian Acoustical Societies Conference, Brisbane, Australia, November 2016, Paper 149.
7. X. Yu, L. Cheng, J.-L. Guyader, Modeling vibroacoustic systems involving cascade open cavities and micro-perforated panels, J. Acoust. Soc. Am. 136, 659–670 (2014).
8. D. Rockwell, E. Naudascher, Review - Self Sustaining Oscillations of Flow Past Cavities, ASME Journal of Engineering 100, 152–165 (1978).
9. P. S. B. Zdanski, M. A. Ortega, G. C. R. Nide, Jr. Fico, Numerical study of the flow over shallow cavities, Computers & Fluids 32, 953–974 (2003).
10. T. M. Faure, P. Adrianos, F. Lusseyran, L. Pastur, Visualizations of the flow inside an open cavity at medium range Reynolds numbers, Experiments in Fluids 42, 169–184 (2007).
11. C. Lada, K. Kontis, Experimental Studies on Transitional and Closed Cavity Configurations Including Flow Control, Journal of Aircraft 47,723–730 (2010)
12. S. Izawa, Active and passive control of flow past a cavity, chapter 17 in: Jorge Colman Lerner and Ulfilas Boldes (Eds.), Wind Tunnel and Experimental Fluid Dynamics Research, InTech Publisher, Shanghai, 2011, pp. 369–394.

13. C. H. Kuo, S. H. Huang, Influence of flow path modification on oscillation of cavity shear layer, Experiments in Fluids 31, 162–178 (2001).
14. M. J. Stanec, J. A. Ross, J. Odedra, J. Peto, High Frequency Acoustic Suppression - The Mystery of the Rod-in-Crossflow Revealed. 41st AIAA Aerospace Sciences Meeting &Exhibit, Reno, USA, AIAA paper 2003-0007, 2003.
15. J. C. F. Pereira, J. M. M. Sousa, Influence of impingement edge geometry on cavity flow oscillations, American Institute of Aeronautics and Astronautics Journal 32 1737–1740 (1994).
16. S. F. McGrath, D. J. Olinger, Control of pressure oscillations in deep cavities excited by grazing flows, Journal of Aircraft 33, 29–36 (1996).
17. D. G. MacManus, D. S. Doran, Passive control of transonic cavity, Journal of Fluids Engineering 130, 1–4 (2008).
18. B. M. Howerton, M. J. Jones, Acoustic Liner Drag: Measurements on Novel Facesheet Perforate Geometries, 16th AIAA/CEAS Aeroacoustics Conference, Lyon, France, AIAA paper 2016-2979, 2016.
19. D. Y. Maa, Microperforated-panel wideband absorber, Noise Control Engineering Journal 29, 77–84 (1997).
20. D. Y. Maa, Potential of microperforated panel absorbers, Journal of the Acoustical Society of America 104, 2861–2866 (1988).
21. B. Fenech, G. Keith, F. Jacobsen, The use of microperforated plates to attenuate cavity resonances, Journal of the Acoustical Society of America 120, 1851–1858 (2006).
22. S. Sack, M. Åbom, Modal filters for mitigation of in-duct sound, Proc. Mtgs. Acoust., 29, 040004 (2016).
23. T. Bravo, C. Maury, C. Pinhède, Absorption and transmission of boundary layer noise through flexible multi-layer micro-perforated structures, Journal of Sound and Vibration 395, 201–223 (2017).
24. M. Goody, Empirical spectral model of surface pressure fluctuations, AIAA J. 42, 1788–1794 (2004).
25. G. M. Corcos, The resolution of pressures in turbulence, J. Acoust. Soc. Am. 35, 192–199 (1963).
26. A. Caiazzo, R. D'Amico, W. Desmet, A generalized Corcos model for modeling turbulent boundary layer wall pressure fluctuations, J. Sound Vib. 372, 192–210 (2016).
27. G. Schewe, On the structure and resolution of wall-pressure fluctuations associated with turbulent boundary layer flow, Journal of Fluid Mechanics 134, 311–328 (1983).
28. J. O. Alvarez, E. J. Kerschen, Influence of Wind Tunnel Walls on Cavity Acoustic Resonances, in: Proceedings of the 11th AIAA/CEAS Aeroacoustics Conference, Monterey, California, U.S.A., May 2005, AIAA 2005-2804.
29. K. Aly, S. Ziada, Flow-excited resonance of trapped modes of ducted shallow cavities, J. Fluids Struct. 26, 92–120 (2010).
30. P. L. Bhatnagar, E. P. Gross, M. A. Krook, A model for collision processes in gases. I. Small amplitude processes in charged and neutral one-component systems, Physical Review 94, 511–525 (1954).